

Tectonic plates in 3D mantle convection model with stress- history-dependent rheology

Takehiro Miyagoshi

Kaiyo Kenkyu Kaihatsu Kiko Yokohama Kenkyujo

Masanori Kameyama (✉ kameyama@sci.ehime-u.ac.jp)

IPU Kantaiheiyu Daigaku Tanki Daigakubu <https://orcid.org/0000-0003-1739-2242>

Masaki Ogawa

Tokyo Daigaku Daigakuin Sogo Bunka Kenkyuka Kyoyo Gakubu

Express Letter

Keywords: Mantle convection, 3D numerical model, Plate Tectonics, Stress-history-dependent rheology

Posted Date: May 15th, 2020

DOI: <https://doi.org/10.21203/rs.3.rs-18967/v2>

License: © ⓘ This work is licensed under a Creative Commons Attribution 4.0 International License.

[Read Full License](#)

Version of Record: A version of this preprint was published on May 24th, 2020. See the published version at <https://doi.org/10.1186/s40623-020-01195-1>.

1 **Tectonic plates in 3D mantle convection model with stress-**
2 **history-dependent rheology**

3 Takehiro Miyagoshi, Japan Agency for Marine-Earth Science and Technology (JAMSTEC),
3173-25 Showa-machi, Kanazawa-ku, Yokohama 236-0001, Japan, miyagoshi@jamstec.go.jp
Masanori Kameyama, Geodynamics Research Center (GRC), Ehime University, 2-5 Bunkyo-
cho, Matsuyama, Ehime 790-8577, Japan, kameyama@sci.ehime-u.ac.jp
Masaki Ogawa, Department of Earth Sciences and Astronomy, University of Tokyo at
Komaba, 3-8-1 Komaba, Meguro, Tokyo 153-8902, Japan, cmaogawa@mail.ecc.u-tokyo.ac.jp

5 **Abstract**

6 Plate tectonics is a key feature of the dynamics of the Earth's mantle. By taking into account the
7 stress-history-dependent rheology of mantle materials, we succeeded in realistically producing tectonic
8 plates in our numerical model of mantle convection in a three-dimensional rectangular box. The
9 calculated lithosphere is separated into several pieces (tectonic plates) that rigidly move. Deformation
10 of the lithosphere caused by the relative motion of adjacent plates is concentrated in narrow bands
11 (plate margins) where the viscosity is substantially reduced. The plate margins develop when the stress
12 exceeds a threshold and the lithosphere is ruptured. Once formed, the plate margins persist, even after
13 the stress is reduced below the threshold, allowing the plates to stably move over geologic time. The
14 vertical component of vorticity takes a large value in the narrow plate margins. Secondary convection
15 occurs beneath old tectonic plates as two-dimensional rolls with their axes aligned to the direction of
16 plate motion. The surface heat flow decreases with increasing distance from divergent plate margins
17 (ridges) in their vicinity in the way the cooling half-space model predicts, but it tends towards a
18 constant value away from ridges as observed for the Earth because of the heat transport by the
19 secondary convection.

20 **Keywords**

21 Mantle convection, 3D numerical model, Plate Tectonics, Stress-history-dependent rheology

22 **Introduction**

23 One of the most challenging issues in studies of the Earth's mantle dynamics is to self-consistently
24 produce tectonic plates in three-dimensional numerical models of mantle convection. The lithosphere
25 develops along the surface boundary, when the viscosity strongly depends on temperature (Weertman
26 1970). The lithosphere produced in this way, however, behaves as a stagnant lid that develops on top of
27 the convecting mantle (Ogawa et al. 1991; Moresi and Solomatov 1995). To allow the lithosphere to be
28 further divided into several pieces (tectonic plates) that rigidly move, it is necessary to introduce plate
29 margins, where the mechanical strength is much lower than that of the surrounding tectonic plates in
30 the lithosphere. In the Earth, plate margins develop when a stress higher than the rupture strength of

31 the lithosphere is induced there by, for example, Large Igneous Provinces (Coffin and Eldholm 1994).
32 Once formed, plate margins persist, even after the stress is reduced below the rupture strength. Indeed,
33 various geophysical and tectonic observations (Kanamori 1980; Zhong and Watts 2013; Gao and Wang
34 2014) show that mechanically weak plate margins persist in the lithosphere at stress levels lower than
35 those for mechanically strong plate interiors. This stress-history-dependent behaviour of the lithosphere
36 is thought to play a crucial role in plate tectonics (Bercovici 1998; Zhong et al. 1998; Ogawa 2003). Here,
37 we present a three-dimensional model of mantle convection to examine how a stress-history-dependent
38 rheology exerts control over the dynamics of the lithosphere.

39 **Methods**

40 The model of mantle convection with tectonic plates was calculated with the ACuTEMan code
41 (Kameyama et al. 2005; Kameyama 2005) as thermal convection of an incompressible Newtonian fluid
42 with an infinite Prandtl number in an internally heated three-dimensional rectangular box with an aspect
43 ratio of 4×4 and a height of 3000 km. The temperature on the surface boundary is fixed at 0° C, whereas
44 the other boundaries are insulating. All of the boundaries are impermeable and shear-stress free. The
45 viscosity strongly depends on the temperature, and the lithosphere develops as the coldest and most
46 viscous part of the cold thermal boundary layer along the surface. The viscosity is also a two-valued
47 function of stress in a range from σ_m (the strength of mechanical coupling at the plate margins) to σ_p
48 (the rupture strength of the lithosphere) (Ogawa 2003). The viscosity takes a high (or “intact”) value
49 for the plate interior when the stress is sufficiently low, but it drops to a low (or “damaged”) value for
50 the plate margins as the stress increases and exceeds σ_p ; the viscosity remains low, even when the stress
51 is reduced below σ_p as long as it is higher than σ_m (see the Additional Materials for more detail). Which
52 of the two values the viscosity takes in the stress range is determined by whether or not the material
53 has experienced a stress higher than σ_p in the past, and this memory of stress-history persists for an
54 indefinitely long period of time as long as σ stays in the range from σ_m to σ_p . We stored this informa-
55 tion of stress history, which is transported by convection, in a scalar quantity called damage parameter
56 (Bercovici et al. 2001; Ogawa 2003). The persistent memory of stress-history of our model is different
57 from the memory assumed in some earlier models (e.g., Bercovici 1998; Foley et al. 2014) that fades
58 away with a decay time of several hundred million years. This persistent memory is the reason why a
59 more plate-like behaviour of the lithosphere is produced in our model. The viscosity for plate interiors

60 is $\eta_p = 10^{27}$ Pa.s, whereas that for plate margins is 3.2×10^{23} Pa.s along the surface boundary. We also
61 assume $\sigma_p = 200$ MPa, a value somewhat lower than earlier estimates (Kohlstedt et al. 1995; Watts and
62 Burov 2003; Jain et al. 2017), and $\sigma_m = 67$ MPa.

63 Results

64 The lithosphere simulated in our model is rifted into several highly viscous pieces (tectonic plates)
65 separated by narrow plate margins where the viscosity is substantially lower than that in the plate interiors
66 (Figure 1a). Each of the plates rigidly moves (see the arrows for velocity vector \mathbf{V} in Figure 1a), and the
67 deformation of the lithosphere caused by relative motion between adjacent plates is accommodated in
68 the narrow plate margins. The cold plates sink into the mantle at convergent plate margins (subduction
69 zones) where $\frac{\partial V_x}{\partial x} + \frac{\partial V_y}{\partial y} < 0$ holds (see the temperature distribution on the vertical section presented
70 in Figure 1a). The vertical component of the vorticity field $(\nabla \times \mathbf{V})_z$ takes a large value in the plate
71 margins except in the subduction zones (Figure 1b); $(\nabla \times \mathbf{V})_z$ is somewhat large over the entire small
72 plate along the west side in Figure 1b too, implying that this plate rigidly rotates. As far as the authors
73 know, Figure 1b is the first example where $(\nabla \times \mathbf{V})_z$ takes a significant value in narrow plate margins in
74 3D numerical models of thermal convection where tectonic plates spontaneously develop (Tackley 2000;
75 Bercovici et al. 2015).

76 The plate motion induces lateral variation in the surface heat flow (Figure 2a). The heat flow decreases
77 with increasing distance L from the divergent plate margins (ridges) in their vicinity. The almost linear
78 dependence of $1/(\text{heat flow})^2$ on L observed in Figure 2b is consistent with a prediction from the cooling
79 half-space model of tectonic plates (Sclater et al. 1980) because L is almost proportional to the surface
80 age because of the calculated stable plate motion in our models (see below).

81 Away from ridges, the value of $1/(\text{heat flow})^2$ deviates from the linear dependence and tends towards
82 a constant value (Figure 2b). Figures 2a and 2c show that the deviation is due to heat transport by
83 the secondary convection that occurs beneath old plates: The distribution of the vertical component of
84 velocity on the horizontal plane at $z = 0.672$ plotted in Figure 2c shows that the secondary convection
85 indeed occurs in the form of two-dimensional rolls whose axes are aligned in the direction of plate motion.
86 The convection rolls extend to the depth of about 1000 km. The secondary convection also induces a
87 stripe pattern in the surface heat flow (Figure 2a). The onset and pattern of secondary convection
88 beneath old oceans are consistent with a prediction from earlier laboratory (Parsons and McKenzie 1978;

89 Richter and Parsons 1975) and numerical (van Hunen et al. 2003; Huang and Zhong 2005) experiments
90 of thermal convection beneath moving plates. Such stripe patterns may be identified in the future by
91 high-resolution tomographic studies of the upper mantle beneath old parts of large oceanic plates such
92 as the Pacific and Indian plates.

93 The time evolution of the velocity distribution along the surface presented in Figure 3 shows that the
94 tectonic plates produced in our model move rather steadily on the non-dimensional time scale of 0.01
95 (or about 3 billion years). Plate A, for example, moves to the southeast, whereas plate B moves to the
96 north, and the ridge between them exists throughout the presented time span. The velocities of these
97 plates do not change so wildly, although the rigid rotation of plate A observed in Figure 3a stops by
98 $t = 5.328 \times 10^{-2}$. The plate margins move in accordance with the plate motion. Ridge R (Figure 3b),
99 for example, moves to the south in frames (b) to (d) because the southward motion of plate C is much
100 faster than the northward motion of plate B.

101 Plate margins persist in our calculation because the lithosphere remembers the location of existing
102 plate margins owing to the assumed stress-history dependence of the viscosity. The margins do not
103 spontaneously disappear; they disappear only when they merge with each other or with the sidewalls of
104 the convecting box owing to the advection by tectonic plates.

105 An interesting feature of the modelled tectonic plates shown in Figure 3 is that the ridges are just simple
106 narrow bands but the subduction zones are more diffuse. Besides, fragments of plates (micro-plates) are
107 often formed along subduction zones (see the area around the southwest and southeast corners of the
108 convecting box). This feature arises because high stress tends to be induced around subduction zones
109 by plate motion. This feature is also observed for the Earth (Gordon et al. 1998). In Figure 3 we could
110 not find a clear relationship between formation of micro-plates and the curvature of plate margins, as
111 opposed to the suggestion by Mallard et al. (2016).

112 Discussion

113 Our model of tectonic plates shown in Figures 1 to 3 indicates that a stress-history-dependent rheology
114 that allows the lithosphere to “remember” the location of plate margins is crucial for plate tectonics to
115 stably operate over geologic time (Zhong et al. 1998; Gurnis et al. 2000). It is difficult to produce stable
116 plate motion together with a large value of $(\nabla \times \mathbf{V})_z$ in narrow plate margins in numerical models where
117 the viscosity depends only on the instantaneous stress (Moresi and Solomatov 1998; Tackley 2000). An

118 example is the yielding model; the lithosphere is intact and its viscosity is high when the stress is less
119 than a threshold, called the yield strength, but it is ruptured and its viscosity is reduced as the stress
120 reaches the threshold. In the yielding model, however, plate margins often spontaneously disappear or
121 migrate at a velocity much higher than the plate velocity as the stress field evolves with time in the
122 lithosphere. Stable motion of tectonic plates separated by narrow plate margins is difficult to produce,
123 even in some models where the viscosity in the lithosphere does depend on its stress history over the past
124 several hundred million years (Foley et al. 2014). See the Additional Materials for more discussion.

125 The stable plate motion produced in our model is important for understanding the global-scale hetero-
126 geneity of the Earth’s mantle revealed by tomographic studies. The large low shear velocity provinces
127 (LLSVPs) develop on the core-mantle boundary away from the slab graveyards where subducted slabs
128 have accumulated over the past several hundred million years (Richards and Engebretson 1992; Cottaar
129 and Lekic 2016). The same feature is observed for numerical models of the evolution of thermo-chemical
130 piles on the core-mantle boundary where the Earth’s plate motion in the past is given as the mechan-
131 ical boundary condition on the surface (Zhang et al. 2010). If plate margins jump and/or migrate so
132 wildly and plate velocity varies with time as strongly as observed in some numerical models where the
133 rheology depends on instantaneous stress rather than stress-history, regions such as LLSVPs and slab
134 graveyards would not have developed (Nakagawa and Tackley 2014). Stable plate motion produced in our
135 model opens a way to self-consistent numerical modelling of the development and evolution of large-scale
136 structures in the Earth’s mantle throughout its history. It is important to further extend our model to
137 three-dimensional spherical geometry of the mantle in future exploration.

138 **Conclusions**

139 In this study we have realistically reproduced for the first time tectonic plates in our model of thermal
140 convection of three-dimensional mantle, by assuming a stress-history-dependent rheology for mantle
141 materials. The tectonic plates calculated in our model show the following five features: (i) rigid motion
142 of cold and stiff plates (both translation and rotation), (ii) accommodation of relative motion of adjacent
143 plates in narrow plate margins, (iii) stable tectonic motions over several billion years, (iv) decrease in
144 surface heat flow in the vicinity of divergent plate boundaries in a way consistent with the prediction
145 from the half-space cooling model, and (v) deviation of the surface heat flow from the half-space cooling
146 model away from divergent plate boundaries. We believe that our model opens a way to self-consistent

147 numerical modelling of development and evolution of large-scale structure in the Earth’s mantle in its
148 history.

149 **List of abbreviations**

150 The large low shear velocity provinces (LLSVPs)

151 **Declarations**

152 **Availability of data and materials**

153 The data that support the findings of this study are available upon reasonable request to T.M. (email:
154 miyagoshi@jamstec.go.jp).

155 The numerical code ACuTEMan is available upon request to M.K. (email: kameyama@sci.ehime-u.ac.jp).

156 **Competing interests**

157 The authors declare no competing interests.

158 **Funding**

159 This work was supported by JSPS KAKENHI Grant Numbers JP25287110, JP15H05834, 18K03724, a
160 joint research program at Geodynamics Research Center, Ehime University, and “Exploratory Challenge
161 on Post-K computer” (Elucidation of the Birth of Exoplanets [Second Earth] and the Environmental
162 Variations of Planets in the Solar System).

163 **Authors’ contributions**

164 T.M. performed numerical simulations, analysis of simulation data, and prepared the manuscript. M.K.
165 developed the numerical simulation code ACuTEMan and prepared the manuscript. M.O. prepared the
166 manuscript. All authors discussed numerical simulation results.

167 **Acknowledgments**

168 This research in part used computational resources of the K computer provided by the RIKEN Center
169 for Computational Science through the HPCI System Research project (Project ID: hp160254,
170 hp170225, hp180199, hp190170).

171 **References**

- 172 Bercovici D (1998) Generation of plate tectonics from lithosphere-mantle flow and void-volatile
173 self-lubrication. *Earth Planet Sci Lett* 154(1-4):139–151, DOI 10.1016/S0012-821X(97)00182-9
- 174 Bercovici D, Ricard Y, Schubert G (2001) A two-phase model for compaction and damage 3.
175 applications to shear localization and plate boundary formation. *J Geophys Res* 106(B5):8925–8939,
176 DOI 10.1029/2000JB900432
- 177 Bercovici D, Tackley PJ, Ricard Y (2015) The generation of plate tectonics from mantle dynamics. In:
178 Schubert G (ed) *Treatise on Geophysics*, vol 7, 2nd edn, Elsevier,
179 DOI 10.1016/B978-0-444-53802-4.00135-4
- 180 Coffin MF, Eldholm O (1994) Large igneous provinces: crustal structure, dimensions, and external
181 consequences. *Rev Geophys* 32(1):1–36, DOI 10.1029/93RG02508
- 182 Cottaar S, Lekic V (2016) Morphology of seismically slow lower-mantle structures. *Geophys J Int*
183 207(2):1122–1136, DOI 10.1093/gji/ggw324
- 184 Foley BJ, Bercovici D, Elkins-Tanton LT (2014) Initiation of plate tectonics from post-magma ocean
185 thermochemical convection. *J Geophys Res Solid Earth* 119(11):8538–8561,
186 DOI 10.1002/2014JB011121
- 187 Gao X, Wang K (2014) Strength of stick-slip and creeping subduction megathrusts from heat flow
188 observations. *Science* 345(6200):1038–1041, DOI 10.1126/science.1255487
- 189 Gordon RG, DeMets C, Royer JY (1998) Evidence for long-term diffuse deformation of the lithosphere
190 of the equatorial Indian Ocean. *Nature* 395(6700):370–374, DOI 10.1038/26463
- 191 Gurnis M, Zhong S, Toth J (2000) On the competing roles of fault reactivation and brittle failure in
192 generating plate tectonics from mantle convection. In: Richards MA, Gordon RG, Van Der Hilst RD
193 (eds) *The History and Dynamics of Global Plate Motions*, Geophysical Monograph, vol 121,
194 American Geophysical Union, pp 73–94, DOI 10.1029/GM121p0073
- 195 Huang J, Zhong S (2005) Sublithospheric small-scale convection and its implications for the residual
196 topography at old ocean basins and the plate model. *J Geophys Res* 110:B05404,
197 DOI 10.1029/2004JB003153
- 198 van Hunen J, Huang J, Zhong S (2003) The effect of shearing on the onset and vigor of small-scale
199 convection in a Newtonian rheology. *Geophys Res Lett* 30(19):1991, DOI 10.1029/2003GL018101
- 200 Jain C, Korenaga J, Karato S (2017) On the yield strength of oceanic lithosphere. *Geophys Res Lett*

201 44(19):9716–9722, DOI 10.1002/2017GL075043

202 Kameyama M (2005) ACuTEMan: A multigrid-based mantle convection simulation code and its
203 optimization to the Earth Simulator. *J Earth Simulator* 4:2–10

204 Kameyama M, Kageyama A, Sato T (2005) Multigrid iterative algorithm using pseudo-compressibility
205 for three-dimensional mantle convection with strongly variable viscosity. *J Comput Phys*
206 206(1):162–181, DOI 10.1016/j.jcp.2004.11.030

207 Kanamori H (1980) The state of stress in the Earth’s lithosphere. In: Dziewonski A, Boschi E (eds)
208 *Physics of the Earth’s Interior*, North-Holland, Amsterdam, pp 531–554

209 Kohlstedt DL, Evans B, Mackwell SJ (1995) Strength of the lithosphere: Constraints imposed by
210 laboratory experiments. *J Geophys Res* 100(B9):17587–17602, DOI 10.1029/95JB01460

211 Mallard C, Coltice N, Seton M, Müller RD, Tackley PJ (2016) Subduction controls the distribution and
212 fragmentation of Earth’s tectonic plates. *Nature* 535(7610):140–143, DOI 10.1038/nature17992

213 Moresi LN, Solomatov V (1995) Numerical investigation of 2D convection with extremely large viscosity
214 variations. *Phys Fluids* 7(9):2154–2162, DOI 10.1063/1.868465

215 Moresi LN, Solomatov V (1998) Mantle convection with a brittle lithosphere: thoughts on the global
216 tectonic styles of the Earth and Venus. *Geophys J Int* 133(3):669–682,
217 DOI 10.1046/j.1365-246X.1998.00521.x

218 Nakagawa T, Tackley PJ (2014) Influence of combined primordial layering and recycled MORB on the
219 coupled thermal evolution of Earth’s mantle and core. *Geochem Geophys Geosyst* 15(3):619–633,
220 DOI 10.1002/2013GC005128

221 Ogawa M (2003) Plate-like regime of a numerically modeled thermal convection in a fluid with
222 temperature-, pressure-, and stress-history-dependent viscosity. *J Geophys Res* 108(B2):2067,
223 DOI 10.1029/2000JB000069

224 Ogawa M, Schubert G, Zebib A (1991) Numerical simulations of three-dimensional thermal convection
225 in a fluid with strongly temperature-dependent viscosity. *J Fluid Mech* 233:299–328,
226 DOI 10.1017/S0022112091000496

227 Parsons B, McKenzie D (1978) Mantle convection and the thermal structure of the plates. *J Geophys*
228 *Res* 83(B9):4485–4496, DOI 10.1029/JB083iB09p04485

229 Richards MA, Engebretson DC (1992) Large-scale mantle convection and the history of subduction.
230 *Nature* 355(6359):437–440, DOI 10.1038/355437a0

231 Richter FM, Parsons B (1975) On the interaction of two scales of convection in the mantle. *J Geophys*
232 *Res* 80(17):2529–2541, DOI 10.1029/JB080i017p02529

233 Slater JG, Jaupart C, Galson D (1980) The heat flow through oceanic and continental crust and the
234 heat loss of the Earth. *Rev Geophys* 18(1):269–311, DOI 10.1029/RG018i001p00269

235 Tackley PJ (2000) Self-consistent generation of tectonic plates in time-dependent, three-dimensional
236 mantle convection simulations 2. strain weakening and asthenosphere. *Geochem Geophys Geosyst*
237 1(8):1026, DOI 10.1029/2000GC000043

238 Watts AB, Burov EB (2003) Lithospheric strength and its relationship to the elastic and seismogenic
239 layer thickness. *Earth Planet Sci Lett* 213(1-2):113–131, DOI 10.1016/S0012-821X(03)00289-9

240 Weertman J (1970) The creep strength of the Earth’s mantle. *Rev Geophys* 8(1):145–168,
241 DOI 10.1029/RG008i001p00145

242 Zhang N, Zhong S, Leng W, Li ZX (2010) A model for the evolution of the Earth’s mantle structure
243 since the Early Paleozoic. *J Geophys Res* 115:B06401, DOI 10.1029/2009JB006896

244 Zhong S, Watts AB (2013) Lithospheric deformation induced by loading of the Hawaiian Islands and its
245 implications for mantle rheology. *J Geophys Res* 118(11):6025–6048, DOI 10.1002/2013JB010408

246 Zhong S, Gurnis M, Moresi L (1998) Role of faults, nonlinear rheology, and viscosity structure in
247 generating plates from instantaneous mantle flow models. *J Geophys Res* 103(B7):15525–15268,
248 DOI 10.1029/98JB00605

Figure 1. The overall three-dimensional structure of thermal convection obtained in our numerical model with stress-history-dependent rheology. (a) The distribution of temperature T in a vertical cross section and that of viscosity η (colour) and velocity \mathbf{V} (arrows) on the surface. The value of η is normalised by η_p , the viscosity of intact material at the surface. (b) The distribution of the vertical component of vorticity $(\nabla \times \mathbf{V})_z$ on the surface.

Figure 2. The lateral variations in the surface heat flow and convecting flow structure. (a) The distribution of the inverse square of the surface heat flow shown in both colour and white contour lines. (b) The plot of the inverse square of heat flow at the surface as a function of the distance L from the divergent plate boundary (ridge) along a horizontal track indicated by the dashed line in (a). Also shown by the dash-dotted line is the theoretical prediction from the half-space cooling for small L , while by the dashed line is the deviation from it for large L . (c) The distribution of vertical component of velocity V_z on the horizontal plane at the height of $z = 0.672$.

Figure 3. The time evolution of the surface plate motions. Snapshots of the distributions of viscosity η (colour) and velocity \mathbf{V} (arrows) in a horizontal plane along the surface at the elapsed times indicated in the figure. The values of η are normalised by η_p , the viscosity of intact material at the surface.

Figures

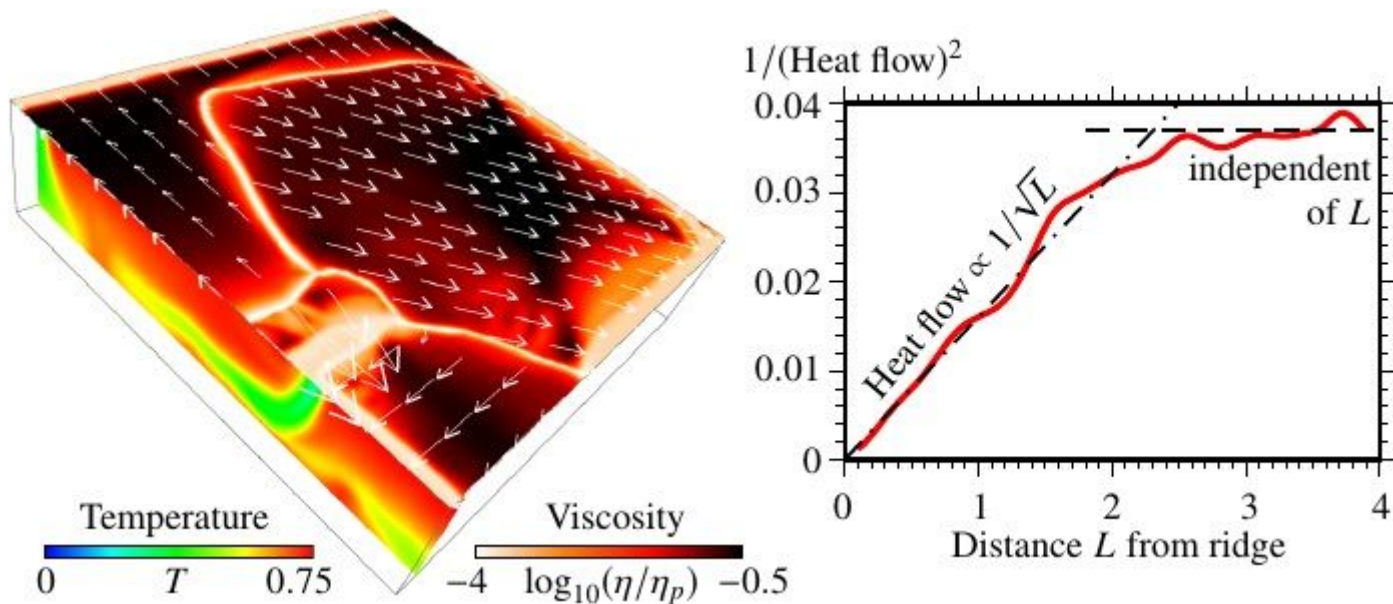


Figure 1

The overall three-dimensional structure of thermal convection obtained in our numerical model with stress-history-dependent rheology. (a) The distribution of temperature T in a vertical cross section and that of viscosity η (colour) and velocity V (arrows) on the surface. The value of η is normalised by η_p , the viscosity of intact material at the surface. (b) The distribution of the vertical component of vorticity $(\nabla \times V)_z$ on the surface.

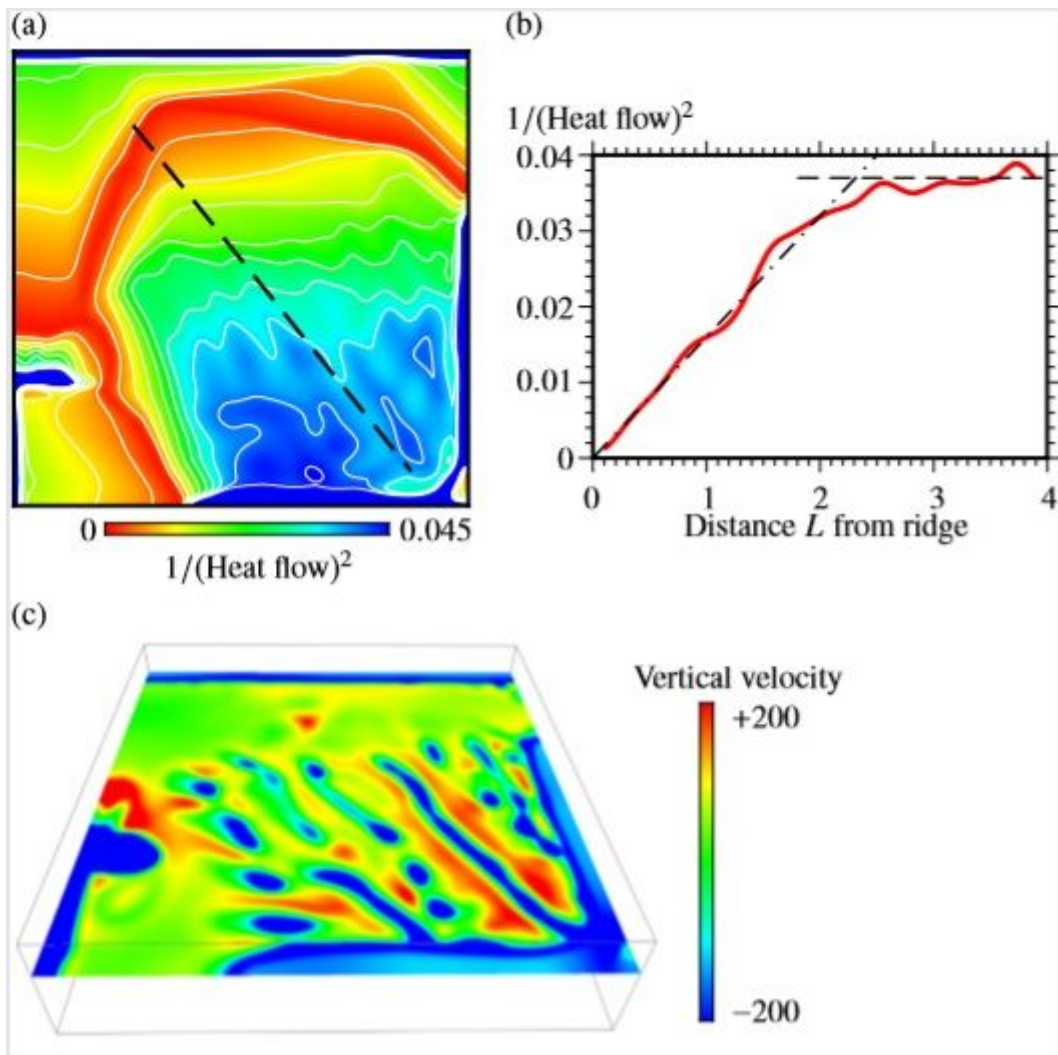


Figure 2

The lateral variations in the surface heat flow and convecting flow structure. (a) The distribution of the inverse square of the surface heat flow shown in both colour and white contour lines. (b) The plot of the inverse square of heat flow at the surface as a function of the distance L from the divergent plate boundary (ridge) along a horizontal track indicated by the dashed line in (a). Also shown by the dash-dotted line is the theoretical prediction from the half-space cooling for small L , while by the dashed line is the deviation from it for large L . (c) The distribution of vertical component of velocity V_z on the horizontal plane at the height of $z = 0.672$.

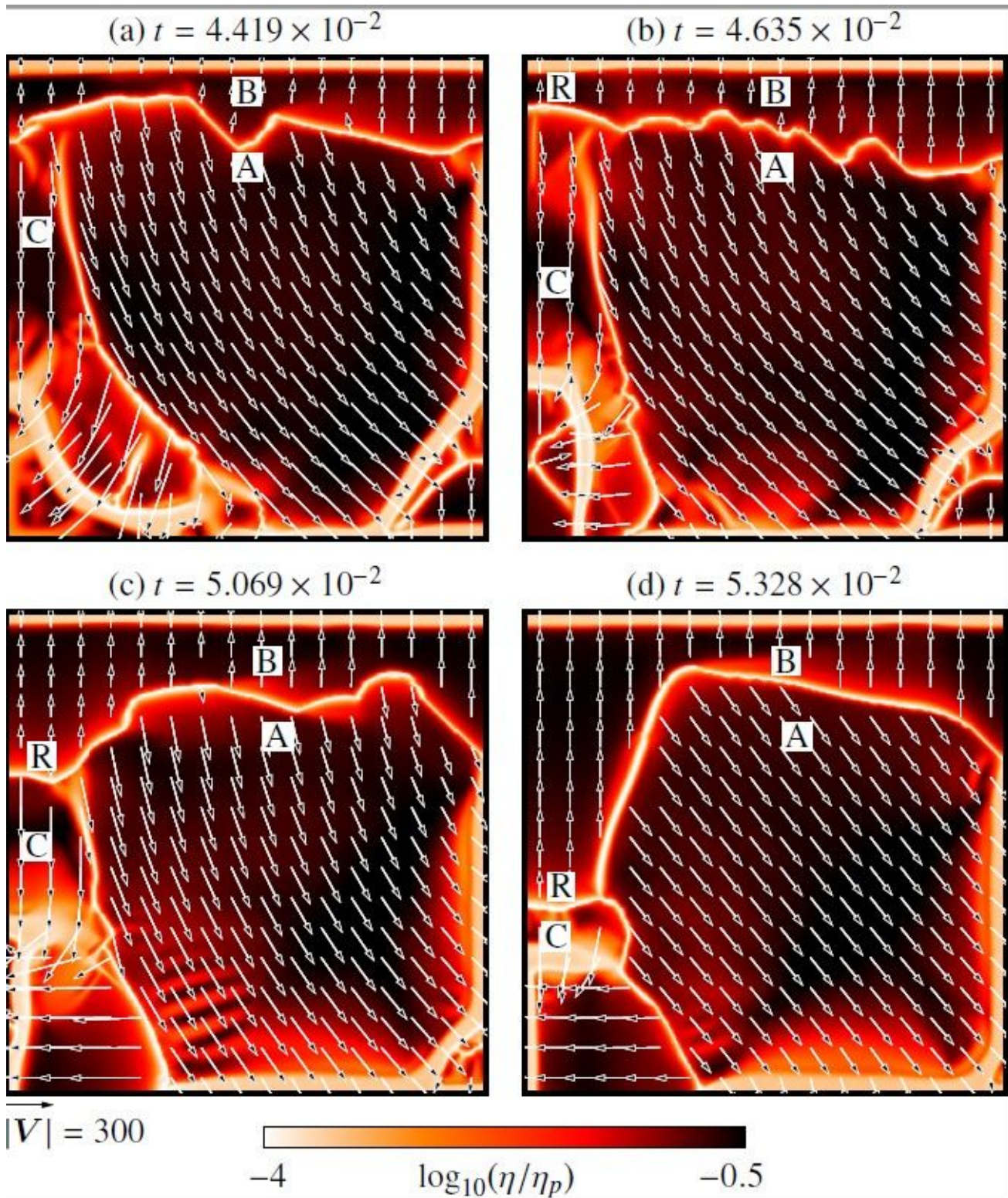


Figure 3

The time evolution of the surface plate motions. Snapshots of the distributions of viscosity η (colour) and velocity V (arrows) in a horizontal plane along the surface at the elapsed times indicated in the figure. The values of η are normalised by η_p , the viscosity of intact material at the surface.

Supplementary Files

This is a list of supplementary files associated with this preprint. Click to download.

- [eps.cls](#)
- [spbasic.bst](#)
- [manuscript4eps.tex](#)
- [gia4eps.png](#)
- [supplement4eps.pdf](#)
- [manuscript4eps.bib](#)